PCCP

PAPER

View Article Online
View Journal | View Issue

Cite this: *Phys. Chem. Chem. Phys.*, 2024, **26**, 15386

Designing potentially singlet fission materials with an anti-Kasha behaviour†

Ricardo Pino-Rios, *[ab] Rodrigo Báez-Grez, [c] Dariusz W. Szczepanik [d] and Miquel Solá *[e]

Received 27th March 2024,
Accepted 2nd May 2024

DOI: 10.1039/d4cp01284d

rsc.li/pccp

Singlet fission (SF) compounds offer a promising avenue for improving the performance of solar cells. Using TD-DFT methods, anti-Kasha azulene derivatives that could carry out SF have been designed. For this purpose, substituted azulenes with a donor (–OH) and/or an acceptor group (–CN) have been systematically studied using the $S_2 \geq 2T_1$ formula. We have found that –CN (–OH) substituents on electrophilic (nucleophilic) carbons result in improved SF properties when compared to azulene.

Introduction

Singlet fission (SF) is a process in which, from light absorption, a chromophore passes from its fundamental state to a singlet excited state, and later, it can collide by diffusion and share its excitation energy with a neighbouring ground state chromophore generating two triplet excited states in a spin-allowed process.[1–4] As a result, from a single photon one can generate two excitons. This phenomenon is exploited in designing new organic compounds with technological, medical, and other applications, the most important being the development of the new generation of solar cells. One of the characteristics that a compound must have in order to be able to perform SF is that it should fulfil the following relation:[5]

$$S_1 \geq 2T_1 \quad (1)$$

Polycyclic aromatic hydrocarbons (PAHs) constitute a popular family of compounds with photoelectronic properties. For example, derivatives of acenes, such as tetracene and pentacene, widely known for their fluorescent properties,[6–8] can carry out SF processes.[9,10] These photoelectronic properties have allowed the development of several derivatives with technological and medical applications.[11]

Additionally, the aromatic character of these PAHs confers stability in the ground state (S_0) and, depending on their delocalization pattern,[12,13] also in the final lowest-lying triplet (T_1) or singlet (S_1) excited state.[14] In this latter group of compounds, stabilization of T_1 explains the low S_0–T_1 gap values of some of these compounds. The S_1 state is involved in photochemical processes only in compounds where Kasha's rule is fulfilled. This rule indicates that the photoelectronic properties, such as fluorescence/phosphorescence, occur in the lowest energy excited state.[15]

A compound well known for its photoelectronic properties is azulene,[16] a naphthalene isomer with a low S_0–T_1 gap and a dipole moment of 1.08 Debye in the ground state.[17] This compound also possesses ten π electrons and, therefore, the compound is globally aromatic according to Platt's perimeter model.[18] Additionally, a local aromatic behaviour is explained in terms of the coexistence of two fused charged rings and the Glidewell–Lloyd rule:[19–21] the tropylium cation and the cyclopentadienyl anion (Scheme 1). Because of this, the negative charge is concentrated on the five-membered ring, allowing it to explain this compound's direction and high dipole moment value.

Another interesting feature of this compound is that it emits through the S_2 excited state in complete violation of Kasha's

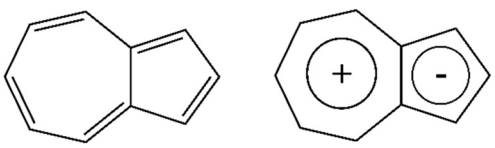

Scheme 1 Proposed covalent (global aromaticity) and ionic (local aromaticity) resonance forms for the ground state of Azulene.

[a] Centro de Investigación Medicina de Altura – CEIMA, Universidad Arturo Prat. Casilla 121, Iquique 1100000, Chile. E-mail: rpinorios@unap.cl
[b] Química y Farmacia, Facultad de Ciencias de la Salud, Universidad Arturo Prat, Casilla 121, Iquique 1100000, Chile
[c] Facultad de Ciencias, Universidad Arturo Prat, Casilla 121, Iquique 1100000, Chile
[d] K. Guminski Department of Theoretical Chemistry, Faculty of Chemistry, Jagiellonian University, Poland
[e] Institut de Química Computacional i Catàlisi (IQCC) and Departament de Química, Universitat de Girona, C/ Maria Aurèlia Capmany 69, 17003 Girona, Catalonia, Spain. E-mail: miquel.sola@udg.edu

† Electronic supplementary information (ESI) available. See DOI: https://doi.org/10.1039/d4cp01284d

rule. It is worth mentioning that this was reported by Michael Kasha himself in his original 1950 paper.[15] Recently, this anomaly has been explained by considering two properties of azulene: first, the excited S_2 state is globally aromatic, giving it stability and a long lifetime allowing the emission from S_2, and, second, there is an easily accessible antiaromaticity relief pathway of the S_1 state.[22]

Research on azulene-containing compounds has once again received considerable attention,[23] with recent work by Casanova *et al.* who integrated two antiparallel azulene units bridged with one heptalene all inserted into a polycyclic conjugated hydrocarbon to design anti-Kasha organic emitters from high excited states.[24]

Moreover, a very detailed study reported by Nickel and Klemp indicates that fluorescence is not the only form of azulene emission since triplet states may also be involved in photochemical processes. The authors indicate that processes such as thermally activated delayed fluorescence (TADF) and SF can take place, with smaller lifetimes and quantum yields, but significant enough to be detected.[25,26]

Computational methods

The construction of the studied compounds was carried out through the systematic substitution of the azulene hydrogens with –OH (π-electron donor) and –CN (π-electron acceptor) groups avoiding the substitution of two rings at the same time in order to understand the influence of the substituents on each of the aromatic rings. A total of 60 systems were designed and optimized to B3LYP[27,28]/6-311G(d,p)[29] in the gas phase, checking that they are local minima on their respective potential energy surfaces. All calculations were performed using the Gaussian 16 program.[30]

Additionally, excited state energies have been studied at the time-dependent density functional theory approach (TD-DFT)[31] level using the same basis set. Since studying the excited states of azulene is not a simple task,[32–34] to obtain reliable energies, a total of 16 functionals were tested, including pure, hybrid, long-range corrected functionals and the Tamm–Dancoff approximation, which is known to correct the triplet instability problems of standard TD-DFT.[35,36] The data obtained were compared with gas-phase experimental data and with DFT/MRCI[37] and CASSCF-NEVPT2[22] calculations reported in the literature. The selection criterion is based not only on the accuracy of the calculations performed with respect to the available data, but also the fact that eqn (2) (S_2–$2T_1$) presents values greater than zero. Another important reason in the selection of the best functional is that the electronic transitions are correctly assigned. For example, experimental reports in conjunction with computational calculations at the DFT/MRCI level indicate that the excited states of interest in this study: T_1, S_1, and S_2 correspond to H → L, H → L, and H−1 → L & H → L+1 transitions, respectively.[38]

The chosen functional (see Table 1) for the calculation of the designed systems is LC-ωHPBE using regular TD-DFT. This functional not only presents reasonable values compared to the experimental data, but also presents a positive value for eqn (2) (1245 cm^{-1}) in full agreement with the experimental results (1000 cm^{-1}). In this case, the values using the Tamm–Dancoff approximation[35] present less accurate values as can be seen in Table S1 in the ESI.†

Table 1 Excited state energy values (in cm^{-1}) computed using regular TD-DFT and the 6-311G(d,p) basis set

	T_1	S_1	S_2	S_2–$2T_1$
Regular TD-DFT	H → L	H → L	H−1 → L; H → L+1	(Eqn (2))
Experimental[37]	13 900	14 300	28 800	1000
DFT/MRCI[38]	14 180	15 400	27 900	−460
CASSCF-NEVPT2[39]	15 383	15 450	31 446	680
B3LYP[27,28]	16 090	19 452	29 418	−2762
BH and HLYP[28,40]	16 696	20 512	30 690	−2701
CAM-B3LYP[41]	15 885	19 516	30 456	−1314
M06[42]	16 146	19 156	28 611	−3682
M06-2X[42]	16 405	19 448	31 313	−1496
M06-HF[43,44]	16 129	18 991	32 544	286
M11L[45]	16 997	19 747	27 640	−6353
BP86[40,46]	15 730	18 885	28 195	−3266
TPSS[47]	16 032	19 355	28 667	−3396
WB97XD[48]	16 048	19 517	30 407	−1689
B97D[49]	15 736	18 938	28 067	−3404
PBE[50]	15 712	18 885	28 263	−3160
PBE0[51]	16 029	19 691	29 976	−2083
HSEH1PBE[52–54]	16 033	19 689	29 872	−2195
LC-BLYP[55]	15 220	19 223	31 191	750
LC-ωHPBE[56]	14 982	19 164	31 208	1245

Results and discussion

The purpose of this article is to take advantage of the characteristics of azulene to design compounds that can carry out SF. For this purpose, we have modified the electronic structure of azulene by systematically replacing hydrogen atoms by π-electron donor groups (–OH) and π-electron acceptor groups (–CN) in positions 1 to 8 (see Fig. 1) obtaining a total of 60 systems that are labelled OH and CN depending on the substituted group followed by the numbers of C atoms to which these substituents are attached (*e.g.* CN4678 means that C atoms number 4, 6, 7, and 8 have a CN substituent and the rest have no substituents). The design of the systems has been carried out systematically, avoiding the substitution of the two rings at the same time in order to evaluate the effect of the substituent per ring.

Since the initial formula given for the design of compounds that can carry out the SF process applies only to those that

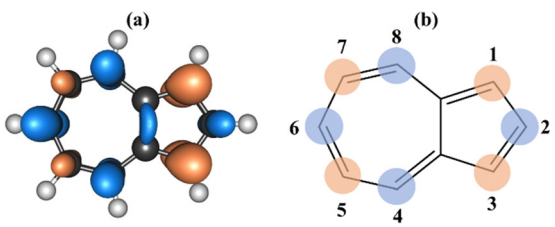

Fig. 1 Dual descriptor (a) and experimental reactivity (b) reported for azulene, including atomic numbering. Orange/blue areas indicate areas susceptible to electrophilic/nucleophilic attack.

comply with Kasha's rule, we have used the following formula to characterize SF chromophores in azulene derivatives:[25]

$$S_2 \geq 2T_1 \quad (2)$$

This equation is used since the emitting excited state in this case is S_2. Because S_2 is higher in energy than S_1, anti-Kasha compounds are more likely to show SF behaviour. First of all, it is necessary to understand the reactivity of azulene in S_0. For this, we have calculated the dual descriptor[57,58] (Fig. 1a), which graphically shows the regions where a compound is more susceptible to nucleophilic/electrophilic attack. The areas in orange are electron-rich areas, which allow the attack of an electrophile, *i.e.* an electron acceptor group, while blue shows the areas prone to nucleophilic attack (electron donor group). These results coincide with the experimentally described reactivity of this compound (Fig. 1b), where the same colour scale is maintained.

The excitation energies of all studied compounds are shown in Table S2 (ESI†). The analysis will be carried out with respect to the unsubstituted compound since it allows understanding the effect of the substituent with respect to the type of carbon

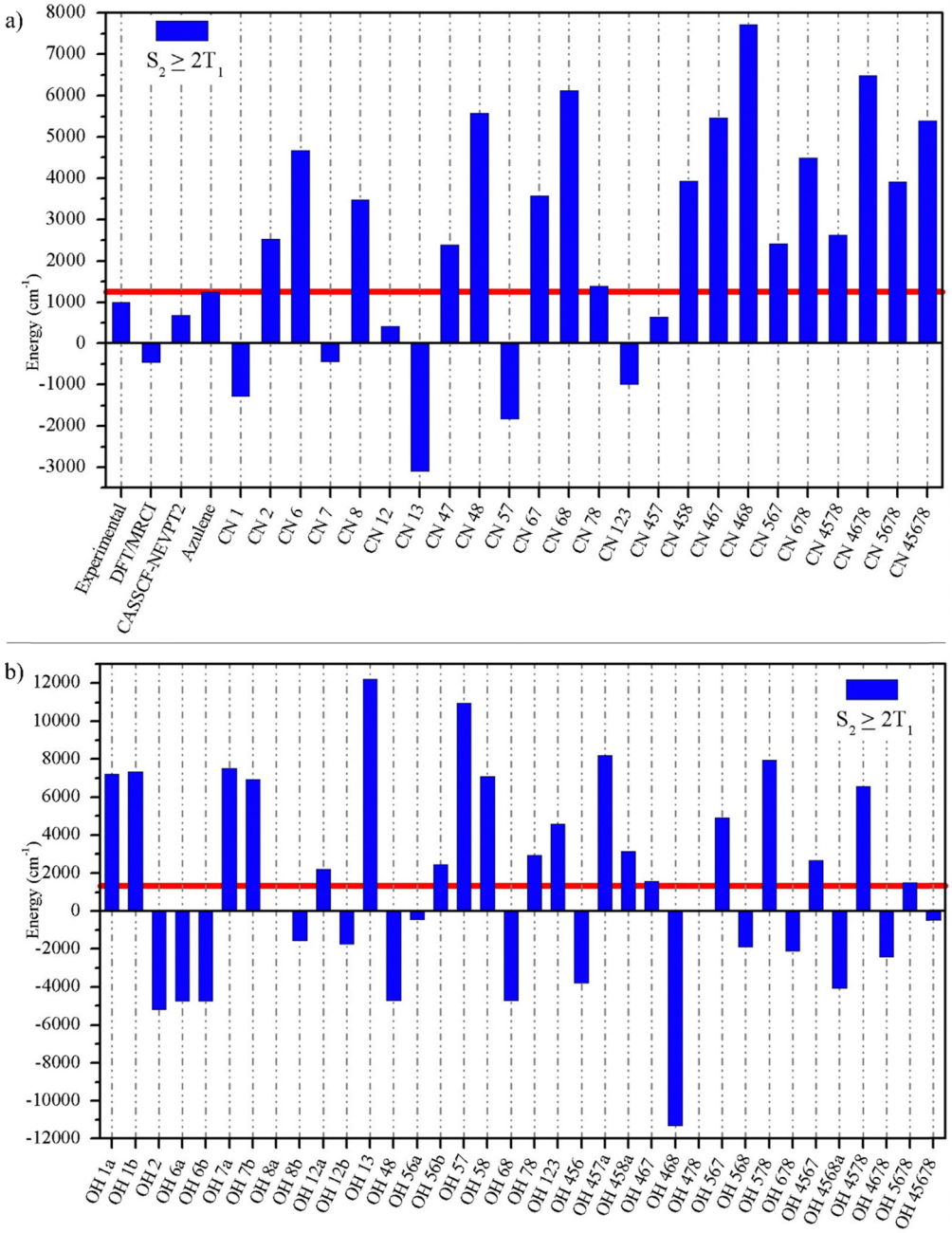

Fig. 2 Computed $S_2 \geq 2T_1$ values for azulene derivatives (a) for substituted –CN compounds and (b) for substituted –OH compounds. The red line corresponds to the value of azulene taken as a reference.

and the corresponding ring in which it has been substituted. We have checked that the nature of the excited states and the frontier molecular orbitals remain the same after substitution (Fig. S1, ESI†). We observe that for the case of the compounds substituted with the –CN group, the effect on the excited states T_1, S_1, and S_2 is mostly stabilizing except for the cases of substitutions in C1 and C2 and those where these two atoms are involved (CN12 and CN123), for which the excited states tend to destabilize when compared to azulene. These exceptions correspond to the five-membered ring atoms.

For the case of those compounds substituted with –OH, the effect of the substituent in the T_1 state is stabilizing on the C1 (C3) and C5 (C7) carbons, which are nucleophilic carbons, while for the case of the electrophilic carbons the effect is clearly destabilizing. With respect to the S_2 state the effect of the substituent is stabilizing only in C1 while, for the other cases, the energies remain practically the same (this is determined by setting a range of ± 1300 cm^{-1} or 0.16 eV).

When we apply eqn (2), it is possible to identify trends that allow us to design SF compounds. In the case of the experimental values reported for azulene, the difference S_2–$2T_1$ has a value of 1000 cm^{-1}, while our results at the TD-LC-ωHPBE/6-311G(d,p)//B3LYP/6-311G(d,p) level give 1245 cm^{-1} in clear agreement with the experimental value, following the same trend, indicating that azulene can act as an SF system. If we apply the formula to literature results obtained at the DFT/MRCI level,[38] we obtain a value of -1700 cm^{-1}, which is clearly underestimated. On the other hand, the values at the CASSCF-NEVPT2 level deviate a little more from the experimental values, however they are in agreement with respect to eqn (2). The value obtained at our level for azulene will serve as a basis for comparison with the results of the substituted systems (see Fig. S2, ESI†).

Fig. 2 shows the results of the application of eqn (2) to the compounds studied. As can be seen, the compounds substituted with –CN are more likely to have positive S_2–$2T_1$ energy gaps, fulfilling the requirements for a SF process to occur. We can note that positive values occur when substitutions have been made on electrophilic carbons (even numbered carbons) and that this influence is maintained in mixed compounds (where both electrophilic and nucleophilic carbons have been replaced). Additionally, it is necessary to mention that the highest values occur when substitutions are made on the 7-membered ring.

Although for both the T_1 and S_2 states the effect of the substituent is similarly stabilizing in almost all cases, the effect in T_1 is more decisive than that of S_2 for the fulfilment of eqn (2). Indeed, compounds that have T_1, S_1, and S_2 stabilized states are more prone to show SF behaviour.

A qualitative explanation of the observed changes can be derived from the dipole moments of the S_0, T_1, S_1, and S_2 states that are 1.04, -0.50, -0.43, and -0.60 Debye, respectively at the B3LYP/6-311G(d,p) level (values for LC-ωHPBE vertical and adiabatic states can be seen in Table S3, ESI†). The direction of the dipole moment in S_0 is justified from Hückel's rule[59,60] and that of T_1 and S_1 by Baird's rule.[61] Therefore, the S_0, and T_1, S_1, and S_2 states have different polarity (Scheme 2). Then,

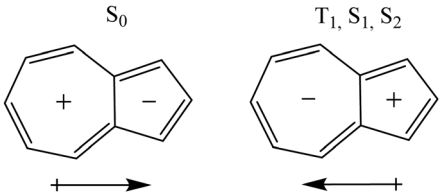

Scheme 2 The different polarity of states S_0, T_1, S_1, and S_2 of azulene. The arrows represent the direction of the dipole moment.

electron acceptor substituents attached to the 7-MR stabilize the T_1, S_1, and S_2 states and destabilize S_0.

Regarding the –OH substituted compounds, although it does not have the same number of systems with positive S_2–$2T_1$, it is the one with the highest value, for example the case of the OH13 (12 216 cm^{-1}) and OH57 (10 996 cm^{-1}) systems. It is also worth mentioning that the effect of the substitution is the inverse of that of –CN. In this case, the positive values occur when the nucleophilic carbons have been substituted.

On the other hand, it is possible to predict the behaviour of the polysubstituted compounds from the values of eqn (2) relative to the azulene of the monosubstituted compounds (see Table 2). The reason for using the relative values concerning azulene is that this compound, although it can perform a SF process, is of very low intensity, so we consider that those that could have a practical effect are those that have values much higher than those of azulene, so that high and positive values relative to this compound will have a greater probability of performing SF.

For example, the S_2–$2T_1$ values relative to the azulene of CN1 and CN2 are -2524 and 1283 cm^{-1}, respectively, while for the case of CN12 it is -831. The sum of the two monosubstituted compounds gives -1240 cm^{-1}, quite close to the calculated value. Additionally, for CN6, CN7, and CN8 the values obtained are 3438, -1691, and 2226 cm^{-1}, respectively. For the case of CN67, CN78, and CN68 the values are 2332, 148, and 4882 cm^{-1}, respectively, very similar to the sum of the values obtained for the monosubstituted compounds. The correlation factor (r^2) between the results obtained from the TD-DFT scheme and those calculated from the sum of the monosubstituted compounds with –CN is 0.97, thus

Table 2 Values obtained for –CN compounds from eqn (2) (relative to azulene) and those obtained from the sum of the monosubstituted compounds (additive approach)

Compound	Eqn (2)[a]	Additive app.	Compound	Eqn (2)[a]	Additive app.
CN12	−831	−1240	CN458	2686	2761
CN13	−4348	−5047	CN467	4217	3972
CN47	1146	535	CN468	6470	7890
CN48	4337	4452	CN567	1179	55
CN57	−3077	−3383	CN678	3250	3972
CN67	2332	1746	CN4578	1378	2281
CN68	4882	5664	CN4678	5243	6198
CN78	148	535	CN5678	2670	2281
CN123	−2237	−3764	CN45678	4155	4507
CN457	−607	−1157			

[a] Values relative to azulene following: $S_{2,X}$–$2T_{1,X}$–$S_{2,azulene}$–$2T_{1,azulene}$, where S_x and T_x represent the respective excited state values for the X designed compound.

allowing to predict results of polysubstituted compounds from those monosubstituted ones (see Fig. S3 and S4 in ESI†).

For those substituted with –OH, the correlation is lower but still significant (r^2 = 0.92, see Table S4 and Fig. S5 and S6 in ESI†). This lower correlation may be due to the formation of intramolecular hydrogen bonds at S_0 thus affecting the values that could be obtained in the vertical excited states.

For the experimental realization of these compounds, it is possible to take advantage of the nucleophilic/electrophilic nature of the azulene carbons and to react them with electrophiles/nucleophiles through aromatic substitution processes. Ideally, the electrophiles/nucleophiles used should be in excess to obtain the polysubstituted compounds.[62,63]

Conclusions

In summary, we have taken advantage of the electronic characteristics of azulene to design anti-Kasha compounds that can carry out singlet fission (SF) processes. For this, we have performed systematic substitutions including π-electron acceptor (–CN) and π-electron donor (–OH) groups and calculations of vertical excited states have been carried out. The formula S_2–$2T_1$ has been used to determine whether a compound can (or cannot) carry out SF processes allowing its application in light harvesting and/or photovoltaics technology. The results obtained indicate that the electron acceptor group (–CN) offers the largest S_2–$2T_1$ values when substitutions were performed on the electrophilic carbons. In the case of monosubstituted compounds, values >4 times higher than azulene were obtained, while in the case of polysubstituted compounds up to >7 times higher. Additionally, it was found that the compounds substituted with the CN group on the electrophilic atoms in the seven-membered ring are the ones that present the best values. On the other hand, the substitutions with the electron donor group (–OH) offer higher values than those of azulene when the substitutions are performed on the nucleophilic carbon atoms regardless of the type of ring.

Finally, it was shown that there is an additive character which would allow predicting the values of S_2–$2T_1$ relative to the azulene of polysubstituted compounds from those of monosubstituted ones. The formula used could obey a more general rule $S_m \geq 2T_n$, where S_m is the relevant singlet state in the process, while T_n is the closest triplet state to it, thus allowing us to predict in a general way compounds that can carry out SF independently of whether or not they fulfil Kasha's rule.

Conflicts of interest

There are no conflicts of interest to declare.

Acknowledgements

This work was supported by the financial support of the National Agency for Research and Development (ANID) through FONDECYT project 1230571 (R. P.-R.). Powered@NLHPC: this research was partially supported by the supercomputing infrastructure of the NLHPC (ECM-02) of the Universidad de Chile. M. S. is grateful for the financial support from the Ministerio de Ciencia e Innovación (Project PID2020-113711GB-I00 MCIN/AEI/10.13039/50110001103) and the Generalitat de Catalunya (Project 2021-SGR-623). D. W. S. acknowledges financial support from the National Science Centre, Poland (2021/42/E/ST4/00332). Open access funding provided by the University of Girona.

References

1 M. B. Smith and J. Michl, Singlet Fission, *Chem. Rev.*, 2010, **110**, 6891–6936.
2 D. Casanova, Theoretical Modeling of Singlet Fission, *Chem. Rev.*, 2018, **118**, 7164–7207.
3 K. Miyata, F. S. Conrad-Burton, F. L. Geyer and X.-Y. Zhu, Triplet Pair States in Singlet Fission, *Chem. Rev.*, 2019, **119**, 4261–4292.
4 T. Ullrich, D. Munz and D. M. Guldi, Unconventional singlet fission materials, *Chem. Soc. Rev.*, 2021, **50**, 3485–3518.
5 A. Japahuge and T. Zeng, Theoretical Studies of Singlet Fission: Searching for Materials and Exploring Mechanisms, *ChemPlusChem*, 2018, **83**, 146–182.
6 A. M. Berghuis, A. Halpin, Q. Le-Van, M. Ramezani, S. Wang, S. Murai and J. Gómez Rivas, Enhanced Delayed Fluorescence in Tetracene Crystals by Strong Light-Matter Coupling, *Adv. Funct. Mater.*, 2019, **29**, 1901317.
7 M. Einzinger, T. Wu, J. F. Kompalla, H. L. Smith, C. F. Perkinson, L. Nienhaus, S. Wieghold, D. N. Congreve, A. Kahn, M. G. Bawendi and M. A. Baldo, Sensitization of silicon by singlet exciton fission in tetracene, *Nature*, 2019, **571**, 90–94.
8 J. Zirzlmeier, D. Lehnherr, P. B. Coto, E. T. Chernick, R. Casillas, B. S. Basel, M. Thoss, R. R. Tykwinski and D. M. Guldi, Singlet fission in pentacene dimers, *Proc. Natl. Acad. Sci. U. S. A.*, 2015, **112**, 5325–5330.
9 M. Dvořák, S. K. K. Prasad, C. B. Dover, C. R. Forest, A. Kaleem, R. W. MacQueen, A. J. I. I. Petty, R. Forecast, J. E. Beves, J. E. Anthony, M. J. Y. Tayebjee, A. Widmer-Cooper, P. Thordarson and T. W. Schmidt, Singlet Fission in Concentrated TIPS-Pentacene Solutions: The Role of Excimers and Aggregates, *J. Am. Chem. Soc.*, 2021, **143**, 13749–13758.
10 C. Zeiser, L. Moretti, F. Reicherter, H. F. Bettinger, M. Maiuri, G. Cerullo and K. Broch, Singlet Fission in Dideuterated Tetracene and Pentacene, *ChemPhotoChem*, 2021, **5**, 758–763.
11 R. Zhang, Y. Guan, Z. Zhu, H. Lv, F. Li, S. Sun and J. Li, Multifunctional Tetracene/Pentacene Host/Guest Nanorods for Enhanced Upconversion Photodynamic Tumor Therapy, *ACS Appl. Mater. Interfaces*, 2019, **11**, 37479–37490.
12 J. Poater, R. Visser, M. Solà and F. M. Bickelhaupt, Polycyclic Benzenoids: Why Kinked is More Stable than Straight, *J. Org. Chem.*, 2007, **72**, 1134–1142.
13 J. Poater, M. Duran and M. Solà, Aromaticity Determines the Relative Stability of Kinked vs. Straight Topologies in Polycyclic Aromatic Hydrocarbons, *Front. Chem.*, 2018, **6**, 561.

14 R. Pino-Rios, R. Báez-Grez and M. Solà, Acenes and phenacenes in their lowest-lying triplet states. Does kinked remain more stable than straight?, *Phys. Chem. Chem. Phys.*, 2021, **23**, 13574–13582.
15 M. Kasha, Characterization of electronic transitions in complex molecules, *Discuss. Faraday Soc.*, 1950, **9**, 14–19.
16 H. Xin, B. Hou and X. Gao, Azulene-Based π-Functional Materials: Design, Synthesis, and Applications, *Acc. Chem. Res.*, 2021, **54**, 1737–1753.
17 T. Kühne, K. H. Au-Yeung, F. Eisenhut, O. Aiboudi, D. A. Ryndyk, G. Cuniberti, F. Lissel and F. Moresco, STM induced manipulation of azulene-based molecules and nanostructures: the role of the dipole moment, *Nanoscale*, 2020, **12**, 24471–24476.
18 J. R. Platt, Classification of Spectra of Cata-Condensed Hydrocarbons, *J. Chem. Phys.*, 2004, **17**, 484–495.
19 C. Glidewell and D. Lloyd, MNDO study of bond orders in some conjugated bi- and tri-cyclic hydrocarbons, *Tetrahedron*, 1984, **40**, 4455–4472.
20 R. Báez-Grez and R. Pino-Rios, Is azulene's local aromaticity and relative stability driven by the Glidewell–Lloyd rule?, *Phys. Chem. Chem. Phys.*, 2024, **26**, 12162–12167.
21 O. El Bakouri, J. Poater, F. Feixas and M. Solà, Exploring the validity of the Glidewell–Lloyd extension of Clar's π-sextet rule: assessment from polycyclic conjugated hydrocarbons, *Theor. Chem. Acc.*, 2016, **135**, 205.
22 D. Dunlop, L. Ludvíková, A. Banerjee, H. Ottosson and T. Slanina, Excited-State (Anti)Aromaticity Explains Why Azulene Disobeys Kasha's Rule, *J. Am. Chem. Soc.*, 2023, **145**, 21569–21575.
23 A. Konishi and M. Yasuda, Breathing New Life into Nonalternant Hydrocarbon Chemistry: Syntheses and Properties of Polycyclic Hydrocarbons Containing Azulene, Pentalene, and Heptalene Frameworks, *Chem. Lett.*, 2021, **50**, 195–212.
24 A. Diaz-Andres, J. Marín-Beloqui, J. Wang, J. Liu, J. Casado and D. Casanova, Rational design of anti-Kasha photoemission from a biazulene core embedded in an antiaromatic/aromatic hybrid, *Chem. Sci.*, 2023, **14**, 6420–6429.
25 B. Nickel and D. Klemp, The lowest triplet state of azulene-h8 and azulene-d8 in liquid solution. I. Survey, kinetic considerations, experimental technique, and temperature dependence of triplet decay, *Chem. Phys.*, 1993, **174**, 297–318.
26 B. Nickel and D. Klemp, The lowest triplet state of azulene-h8 and azulene-d8 in liquid solution.: II. Phosphorescence and E-type delayed fluorescence, *Chem. Phys.*, 1993, **174**, 319–330.
27 A. D. Becke, Becke's three parameter hybrid method using the LYP correlation functional, *J. Chem. Phys.*, 1993, **98**, 5648–5652.
28 C. Lee, W. Yang and R. G. Parr, Development of the Colle-Salvetti correlation-energy formula into a functional of the electron density, *Phys. Rev. B: Condens. Matter Mater. Phys.*, 1988, **37**, 785–789.
29 R. Ditchfield, W. J. Hehre and J. A. Pople, Self-Consistent Molecular-Orbital Methods. IX. An Extended Gaussian-Type Basis for Molecular-Orbital Studies of Organic Molecules, *J. Chem. Phys.*, 1971, **54**, 724–728.
30 M. J. Frisch, G. W. Trucks, H. B. Schlegel, G. E. Scuseria, M. A. Robb, J. R. Cheeseman, G. Scalmani, V. Barone, G. A. Petersson, H. Nakatsuji, X. Li, M. Caricato, A. V. Marenich, J. Bloino, B. G. Janesko, R. Gomperts, B. Mennucci, H. P. Hratchian, J. V. Ortiz, A. F. Izmaylov, J. L. Sonnenberg, D. Williams-Young, F. Ding, F. Lipparini, F. Egidi, J. Goings, B. Peng, A. Petrone, T. Henderson, D. Ranasinghe, V. G. Zakrzewski, J. Gao, N. Rega, G. Zheng, W. Liang, M. Hada, M. Ehara, K. Toyota, R. Fukuda, J. Hasegawa, M. Ishida, T. Nakajima, Y. Honda, O. Kitao, H. Nakai, T. Vreven, K. Throssell, J. A. Montgomery Jr., J. E. Peralta, F. Ogliaro, M. J. Bearpark, J. J. Heyd, E. N. Brothers, K. N. Kudin, V. N. Staroverov, T. A. Keith, R. Kobayashi, J. Normand, K. Raghavachari, A. P. Rendell, J. C. Burant, S. S. Iyengar, J. Tomasi, M. Cossi, J. M. Millam, M. Klene, C. Adamo, R. Cammi, J. W. Ochterski, R. L. Martin, K. Morokuma, O. Farkas, J. B. Foresman and D. J. Fox, *Gaussian 16, Rev. B.01*, Gaussian, Inc., Wallingford CT, 2016.
31 C. Ullrich, *Time-Dependent Density-Functional Theory: Concepts and Applications*, OUP, Oxford, 2012.
32 K. Veys and D. Escudero, Computational Protocol To Predict Anti-Kasha Emissions: The Case of Azulene Derivatives, *J. Phys. Chem. A*, 2020, **124**, 7228–7237.
33 A. Murakami, T. Kobayashi, A. Goldberg and S. Nakamura, CASSCF and CASPT2 studies on the structures, transition energies, and dipole moments of ground and excited states for azulene, *J. Chem. Phys.*, 2004, **120**, 1245–1252.
34 K. Veys and D. Escudero, Anti-Kasha Fluorescence in Molecular Entities: Central Role of Electron–Vibrational Coupling, *Acc. Chem. Res.*, 2022, **55**, 2698–2707.
35 S. Hirata and M. Head-Gordon, Time-dependent density functional theory within the Tamm–Dancoff approximation, *Chem. Phys. Lett.*, 1999, **314**, 291–299.
36 M. J. G. Peach, M. J. Williamson and D. J. Tozer, Influence of Triplet Instabilities in TDDFT, *J. Chem. Theory Comput.*, 2011, **7**, 3578–3585.
37 R. P. Steer, Photophysics of molecules containing multiples of the azulene carbon framework, *J. Photochem. Photobiol., C*, 2019, **40**, 68–80.
38 S. Vosskötter, P. Konieczny, C. M. Marian and R. Weinkauf, Towards an understanding of the singlet–triplet splittings in conjugated hydrocarbons: Azulene investigated by anion photoelectron spectroscopy and theoretical calculations, *Phys. Chem. Chem. Phys.*, 2015, **17**, 23573–23581.
39 Y. Guo, K. Sivalingam, E. F. Valeev and F. Neese, SparseMaps—A systematic infrastructure for reduced-scaling electronic structure methods. III. Linear-scaling multireference domain-based pair natural orbital N-electron valence perturbation theory, *J. Chem. Phys.*, 2016, **144**, 94111.
40 A. D. Becke, Density-functional exchange-energy approximation with correct asymptotic behavior, *Phys. Rev. A: At., Mol., Opt. Phys.*, 1988, **38**, 3098–3100.
41 T. Yanai, D. P. Tew and N. C. Handy, A new hybrid exchange–correlation functional using the Coulomb-attenuating method (CAM-B3LYP), *Chem. Phys. Lett.*, 2004, **393**, 51–57.

42 Y. Zhao and D. G. Truhlar, The M06 suite of density functionals for main group thermochemistry, thermochemical kinetics, noncovalent interactions, excited states, and transition elements: two new functionals and systematic testing of four M06-class functionals and 12 other functionals, *Theor. Chem. Acc.*, 2008, **120**, 215–241.
43 Y. Zhao and D. G. Truhlar, Comparative DFT Study of van der Waals Complexes: Rare-Gas Dimers, Alkaline-Earth Dimers, Zinc Dimer, and Zinc-Rare-Gas Dimers, *J. Phys. Chem. A*, 2006, **110**, 5121–5129.
44 Y. Zhao and D. G. Truhlar, Density Functional for Spectroscopy: No Long-Range Self-Interaction Error, Good Performance for Rydberg and Charge-Transfer States, and Better Performance on Average than B3LYP for Ground States, *J. Phys. Chem. A*, 2006, **110**, 13126–13130.
45 R. Peverati and D. G. Truhlar, M11-L: A Local Density Functional That Provides Improved Accuracy for Electronic Structure Calculations in Chemistry and Physics, *J. Phys. Chem. Lett.*, 2012, **3**, 117–124.
46 J. P. Perdew, Density-functional approximation for the correlation energy of the inhomogeneous electron gas, *Phys. Rev. B: Condens. Matter Mater. Phys.*, 1986, **33**, 8822–8824.
47 J. Tao, J. P. Perdew, V. N. Staroverov and G. E. Scuseria, Climbing the Density Functional Ladder: Nonempirical Meta – Generalized Gradient Approximation Designed for Molecules and Solids, *Phys. Rev. Lett.*, 2003, **91**, 146401.
48 J.-D. Chai and M. Head-Gordon, Long-range corrected hybrid density functionals with damped atom–atom dispersion corrections, *Phys. Chem. Chem. Phys.*, 2008, **10**, 6615–6620.
49 S. Grimme, Semiempirical GGA-type density functional constructed with a long-range dispersion correction, *J. Comput. Chem.*, 2006, **27**, 1787–1799.
50 J. P. Perdew, K. Burke and M. Ernzerhof, Generalized Gradient Approximation Made Simple, *Phys. Rev. Lett.*, 1996, **77**, 3865–3868.
51 C. Adamo and V. Barone, Toward reliable density functional methods without adjustable parameters: The PBE0 model, *J. Chem. Phys.*, 1999, **110**, 6158–6170.
52 J. Heyd and G. E. Scuseria, Efficient hybrid density functional calculations in solids: Assessment of the Heyd–Scuseria–Ernzerhof screened Coulomb hybrid functional, *J. Chem. Phys.*, 2004, **121**, 1187–1192.
53 J. Heyd and G. E. Scuseria, Assessment and validation of a screened Coulomb hybrid density functional, *J. Chem. Phys.*, 2004, **120**, 7274–7280.
54 J. Heyd, J. E. Peralta, G. E. Scuseria and R. L. Martin, Energy band gaps and lattice parameters evaluated with the Heyd-Scuseria-Ernzerhof screened hybrid functional, *J. Chem. Phys.*, 2005, **123**, 174101.
55 H. Iikura, T. Tsuneda, T. Yanai and K. Hirao, A long-range correction scheme for generalized-gradient-approximation exchange functionals, *J. Chem. Phys.*, 2001, **115**, 3540–3544.
56 T. M. Henderson, A. F. Izmaylov, G. Scalmani and G. E. Scuseria, Can short-range hybrids describe long-range-dependent properties?, *J. Chem. Phys.*, 2009, **131**, 44108.
57 C. Morell, A. Grand and A. Toro-Labbé, New Dual Descriptor for Chemical Reactivity, *J. Phys. Chem. A*, 2005, **109**, 205–212.
58 R. Pino-Rios, D. Inostroza, G. Cárdenas-Jirón and W. Tiznado, Orbital-Weighted Dual Descriptor for the Study of Local Reactivity of Systems with (Quasi-) Degenerate States, *J. Phys. Chem. A*, 2019, **123**, 10556–10562.
59 E. Hückel, Quanstentheoretische Beiträge zum Benzolproblem, *Z. Phys.*, 1931, **72**, 310–337.
60 H. Möllerstedt, M. C. Piqueras, R. Crespo and H. Ottosson, Fulvenes, Fulvalenes, and Azulene: Are They Aromatic Chameleons?, *J. Am. Chem. Soc.*, 2004, **126**, 13938–13939.
61 N. C. Baird, Quantum organic photochemistry. II. Resonance and aromaticity in the lowest 3.pi..pi.* state of cyclic hydrocarbons, *J. Am. Chem. Soc.*, 1972, **94**, 4941–4948.
62 A. C. Razus, Azulene, Reactivity, and Scientific Interest Inversely Proportional to Ring Size; Part 1: The Five-Membered Ring, *Symmetry*, 2023, **15**, 310.
63 A. C. Razus, Azulene, Reactivity, and Scientific Interest Inversely Proportional to Ring Size; Part 2: The Seven-Membered Ring, *Symmetry*, 2023, **15**, 1391.

